

# Development of Al–Mg–Si alloy performance by addition of grain refiner Al–5Ti–1B alloy

Science Progress

2021, Vol. 104(2) 1–15

© The Author(s) 2021

Article reuse guidelines:

[sagepub.com/journals-permissions](https://sagepub.com/journals-permissions)

DOI: 10.1177/00368504211029469

[journals.sagepub.com/home/sci](https://journals.sagepub.com/home/sci)

Khaled Abd El-Aziz<sup>1</sup>, Emad M Ahmed<sup>2</sup>, Abdulaziz H Alghtani<sup>1</sup>, Bassem F Felemban<sup>1</sup>, Hafiz T Ali<sup>1</sup> , Mona Megahed<sup>3</sup> and Dalia Saber<sup>4</sup> 

<sup>1</sup>Department of Mechanical Engineering, College of Engineering, Taif University, Taif, Saudi Arabia

<sup>2</sup>Department of Physics, College of Science, Taif University, Taif, Saudi Arabia

<sup>3</sup>Department of Mechanical Design and Production Engineering, Faculty of Engineering, Zagazig University, Zagazig, Egypt

<sup>4</sup>Industrial Engineering Program, Department of Mechanical Engineering, College of Engineering, Taif University, Taif, Saudi Arabia

## Abstract

Aluminum alloys are the most essential part of all shaped castings manufactured, mainly in the automotive, food industry, and structural applications. There is little consensus as to the precise relationship between grain size after grain refinement and corrosion resistance; conflicting conclusions have been published showing that reduced grain size can decrease or increase corrosion resistance. The effect of Al–5Ti–1B grain refiner (GR alloy) with different percentages on the mechanical properties and corrosion behavior of Aluminum-magnesium-silicon alloy (Al–Mg–Si) was studied. The average grain size is determined according to the E112ASTM standard. The compressive test specimens were made as per ASTM: E8/E8M-16 standard to get their compressive properties. The bulk hardness using Vickers hardness testing machine at a load of 50g. Electrochemical corrosion tests were carried out in 3.5 % NaCl solution using Autolab Potentiostat/Galvanostat (PGSTAT 30). The grain size of the Al–Mg–Si alloy was reduced from 82 to 46  $\mu\text{m}$  by the addition of GR alloy. The morphology of  $\alpha$ -Al dendrites changes from coarse dendritic structure to fine equiaxed grains due to the addition of GR alloy and segregation of Ti, which controls the growth of primary  $\alpha$ -Al. In addition, the mechanical properties of the Al–Mg–Si alloy were improved by GR alloy addition. GR alloy addition to Al–Mg–Si alloy produced fine-

## Corresponding author:

Dalia Saber, Industrial Engineering Program, Department of Mechanical Engineering, College of Engineering, Taif University, P.O. Box 11099, Taif 21944, Saudi Arabia.

Emails: [dselsayed@tu.edu.sa](mailto:dselsayed@tu.edu.sa); [daliasaber13@yahoo.com](mailto:daliasaber13@yahoo.com)



Creative Commons Non Commercial CC BY-NC: This article is distributed under the terms of the Creative Commons Attribution-NonCommercial 4.0 License (<https://creativecommons.org/licenses/by-nc/4.0/>)

which permits non-commercial use, reproduction and distribution of the work without further permission provided the original work is attributed as specified on the SAGE and Open Access pages (<https://us.sagepub.com/en-us/nam/open-access-at-sage>).

grained structure and better hardness and compressive strength. The addition of GR alloy did not reveal any marked improvements in the corrosion properties of Al–Mg–Si alloy.

### Keywords

Al–Mg–Si alloy, food industry, Al–Ti–B grain refiner, hardness, corrosion behavior, compression test

## Introduction

Aluminum alloys cookware, cooking utensil, containers, and aluminum drink jars contribute significantly to the utilization mass of aluminum. The finest combination of corrosion resistance and strength for user application in wrought aluminum products is found amongst the 5xxx and 6xxx series alloys.<sup>1</sup> Furthermore, several casting alloys have good corrosion resistance, and they are commonly used as cooking utensils and components of food processing equipment.<sup>2</sup> Al alloys with mechanical properties, good weldability, and good corrosion resistance characteristics.<sup>3–6</sup> Traditional aluminum alloys face the difficulties of coarse grains after casting and solidification. Coarse grains, seriously affect the mechanical properties of aluminum alloy. They frequently cause defects, such as composition segregation, cracks, and shrinkage cavities. Consequently, the grain refinement addition of Al alloys to improve the mechanical properties and the microstructure of Al alloys has become a research focus<sup>7</sup>

Kodetová, et al.<sup>8</sup> concluded that the addition of Sc, Zr in the hot-rolled alloys stabilizes and refines grains. The grain size was around 1000  $\mu\text{m}$  in the AlZnMgCuFe and change to 20  $\mu\text{m}$  in the AlZnMgCuFeScZr hot-rolled alloys. Zhang et al.<sup>9</sup> obvious that the addition of a small amount of titanium (less than 0.10 wt.%) to the alloy Al–Mg–Zn–Si lead to the formation of the  $\text{Al}_3\text{Ti}$  phase, and enhanced the mechanical properties of this alloy. Abd El-Aziz et al.<sup>10</sup> studied the effect of the addition a different ratio (0–3 wt.%) of Al–5Ti master alloy on the microstructure and mechanical properties of AlSiMgMn alloy. They established that 2 wt.% addition of Al–5Ti increased the ultimate tensile strength of the alloy from 165 to 208 MPa and the yield strength from 125 to 160 MPa respectively. On the other hand, 3 wt.% addition of Al–5Ti master alloy did not reveal any noticeable improvements in these properties. Ding et al.<sup>11</sup> studied the effect of different types of Al–5Ti master alloys that have different microstructures in grain refinement of commercial aluminum. They decided that the microstructures details of Al–5Ti master alloys with various sizes, morphologies, and amounts of  $\text{TiAl}_3$  intermetallic, were detected to affect the arrangement of the grain refinement characteristics with the right holding time. Pio et al.<sup>12</sup> examined the effect of the addition of Al–5Ti–B master alloy on the mechanical properties of LM6 Al–Si alloy. The typical LM6 Al alloy contains 10–13 wt.% of Si and thus integrally solidifies with coarse grain sizes. The results exposed that the improvement of mechanical properties of the alloy by grain refiner by 0.5 wt.% Al–5Ti–B master alloy addition. On the other hand, a further increase in grain refiner quantity did not afford any additional noteworthy improvement.

Most of the previous studies on the effect of grain refinement of Al alloys have mainly focused on mechanical properties. On the other hand, there are some studies investigate the relationship between grain size after grain refinement and corrosion resistance. Conflicting conclusions have been published showing that reduced grain size can decrease or increase corrosion resistance.<sup>13</sup> Ralston and Birbilis<sup>14</sup> revised the effect of grain size on corrosion performance. They suggested that an increase or decrease in corrosion resistance of the alloy with grain refinement depends on the ability of the environment to passivate the alloy. In an active environment, reduced grain size leads to a decrease in corrosion resistance. However, in the environment's hopeful passivity, reduced grain size may lead to an increase in corrosion resistance. In this study, the effect of the different percentages of Al-5Ti-1B grain refiner (GR alloy) on the microstructure and mechanical properties as well as corrosion properties of Al-Mg-Si alloy was investigated.

## Experimental work

The materials in this study are Al-Mg-Si alloy and Al-5Ti-1B grain refiner (GR alloy) with different percentages. The base Aluminum-magnesium-silicon alloy used in the present study contains 1.2% Si, 0.93% Mg, 0.7% Mn, and 0.4% Fe. The specimens were fabricated by the die casting method. Al-Mg-Si alloy was melted in a crucible furnace at 750°C. Al-5Ti-1B grain refiner with different weight percentages of 0, 1, 1.5, and 2 wt.% was added to the melt. The melt was poured into metallic steel molds. After the casting process the specimens are prepared for microstructural examination, mechanical, and corrosion tests. The test specimens are ground and polished using SiC abrasive emery papers, ranged from 180 to 1200 grit size. For microstructural examination, the polished specimens were etched by a reagent contains 75 ml HCl, 25 ml HNO<sub>3</sub>, 5 ml HF, and 25 ml H<sub>2</sub>O to reveal their microstructure constituents. The microstructures were examined using an optical microscope, a scanning electron microscope (SEM) equipped with an energy dispersive X-ray spectrometer (EDS). The average grain size is determined according to the E112ASTM standard. The as-cast compressive test specimens were made as per ASTM: E8/E8M-16 standard to get their compressive properties. The compression tests are conducted on round test specimens at a diameter of 15mm and a height of 15mm using a universal testing machine. The bulk hardness was measured on the specimens after grinding and polishing using a Vickers hardness testing machine at a load of 50 g. Each value of the bulk hardness was an average of five readings.

Electrochemical corrosion tests were carried out in 3.5 wt.% NaCl solution using Autolab Potentiostat/Galvanostat (PGSTAT 30). In the electrochemical testing, a cell with three-electrode was used. The working electrode was the test specimen; the auxiliary electrode was a platinum rod and the reference electrode was a saturated calomel electrode. Prior to testing samples were immersed in the testing solution until attaining a steady-state corrosion potential ( $E_{\text{corr}}$ ). Potentiodynamic polarization curves were measured in the range  $-0.4$  to  $1$  V with respect to  $E_{\text{corr}}$  at a scan

rate of  $2 \text{ mVs}^{-1}$  and  $20^\circ\text{C}$ . The area of the working electrode exposed to the solution was  $0.785 \text{ cm}^2$ . Electrochemical impedance spectroscopy (EIS) measurements were executed using scan frequency ranged from 60 kHz to 1 Hz, and the perturbation amplitude was 10 mV. After the corrosion test, the microstructures of the corroded surface were examined using an optical microscope.

## Results and discussion

### Microstructure

Figure 1 shows SEM images and EDS analysis for the Al–Mg–Si alloy and GR alloy used in the present study. As shown in Figure 1(a), the as-cast microstructure of the Al–Mg–Si alloy consists of  $\alpha$ -Al dendrites and inter-dendritic regions of the eutectic phase formed between  $\alpha$ -Al dendrites. Figure 1(b) presents EDS spectrum of the elements at different zones in the microstructure of Al–Mg–Si alloy. From this figure, it can be seen that the presence of small peaks of the Mg and Si elements as well as the presence of a big peak of the parent element of Al. Figures 1(c) and (d) indicate SEM/EDS spectrum analysis for GR alloy. The SEM photograph of the Al–5Ti–1B grain refiner alloy is shown in Figure 1(c). It can be seen that the second phase particles of  $\text{TiAl}_3$  and  $\text{TiB}_2$  are dispersed in the aluminum matrix homogeneously. As also illustrated in this figure, the particles are disconnected from each other with various sizes. EDS spectrum results in Figure 1(d), reveals the existence of smaller amounts of Ti and B elements in the microstructure of Al–5Ti–1B grain refiner. Figure 2 displays an XRD plot of GR alloy that confirms the phases present in the microstructure. As indicated in the XRD pattern shown in Figure 2, it is obvious that the grain refiner alloy primarily contains three kinds of phases:  $\alpha$ -Al,  $\text{TiAl}_3$ , and  $\text{TiB}_2$ . The as-cast microstructure of the base Al–Mg–Si alloy with 0, 1, 1.5, and 2 wt.% of GR alloy is shown in the optical micrographs in Figure 3. As shown in Figure 3(a), the as-cast microstructure of Al–Mg–Si alloy reveals coarse dendrites of  $\alpha$ -Al phase. The adding of GR alloy to Al–Mg–Si alloy caused alterations in the morphology of the  $\alpha$ -Al phase from coarse dendrites to relatively small dendrites and fine equiaxed microstructure as shown in Figure 3(b) to (d). It is also clear that the grain size decreases with the increase of the quantity of the GR alloy, and smaller sizes of grains were observed for the Al–Mg–Si alloy with 2 wt.% of GR alloy. This confirms the uniform distribution of insoluble substrates in the Al-matrix, which acts as nucleation sites for the primary  $\alpha$ -Al phase.

### Compression test

The compressive strength can be estimated more correctly than tensile strength in the cast condition. Because of the porosity present in the cast alloy, it would produce an inaccurate result in tensile strength. While the porosity of the alloy would not influence the compressive strength due to compressive force applied on the tested materials. Figure 4 shows the compressive strength and grain size variations

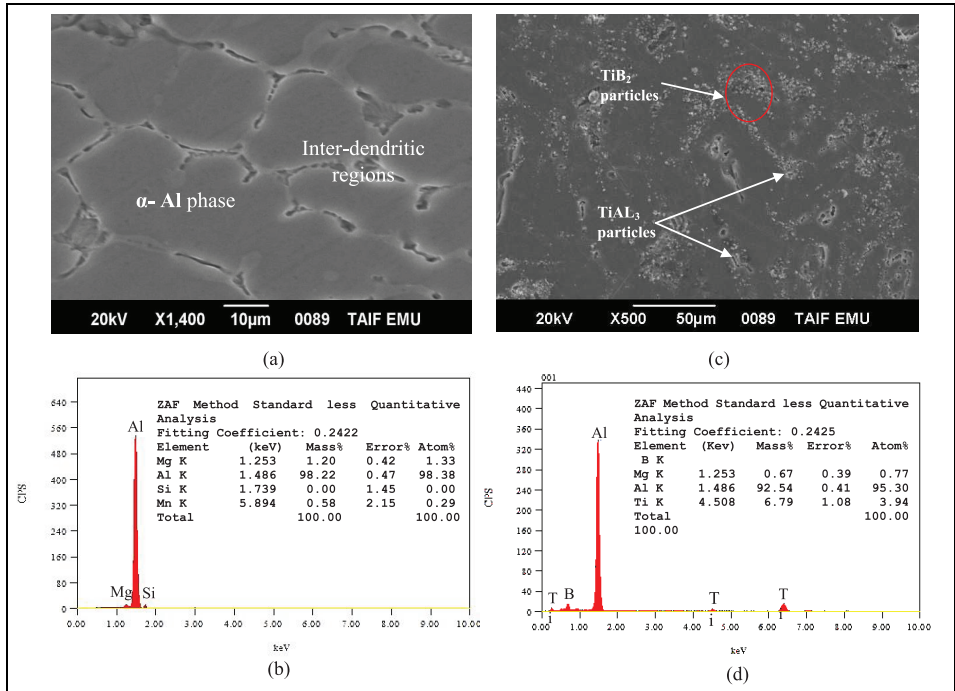


Figure 1. (a), (b) SEM/EDS spectrum for the Al–Mg–Si alloy used in the present study and (c), (d) SEM/EDS spectrum for the Al–5Ti–1B grain refiner.

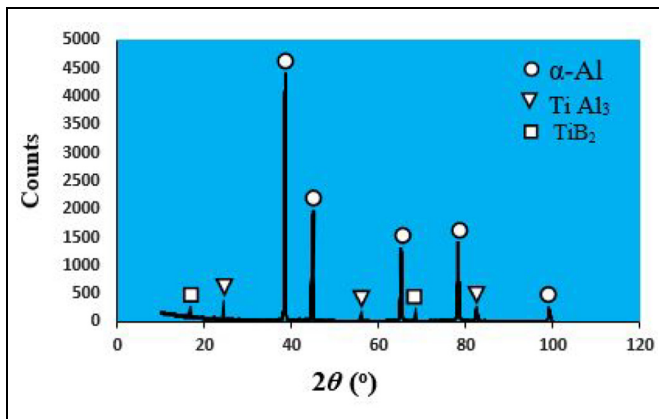
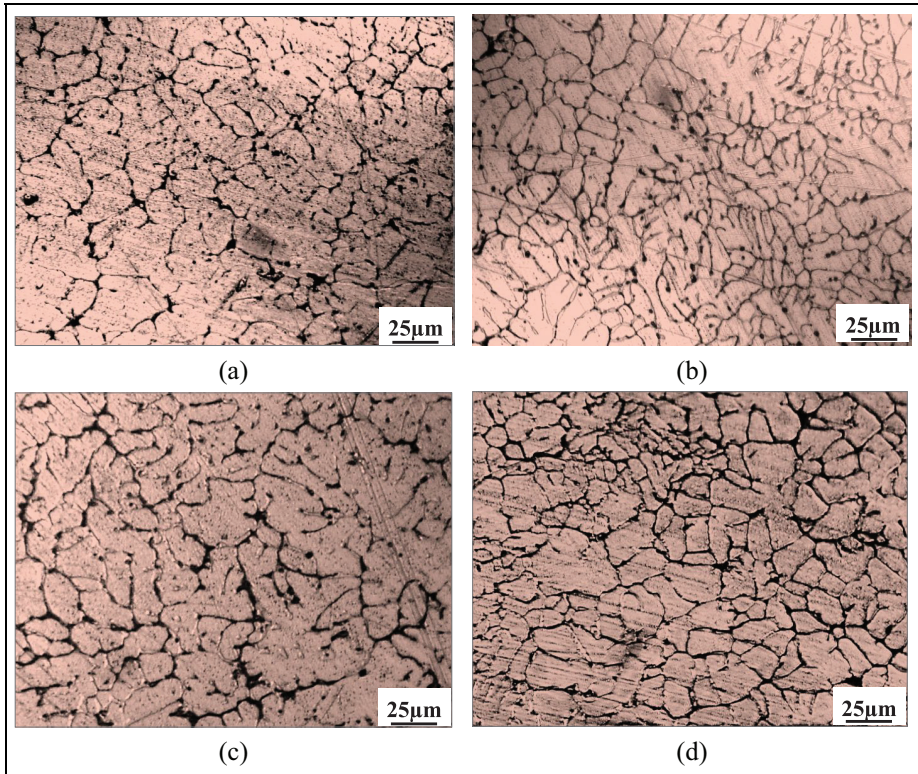
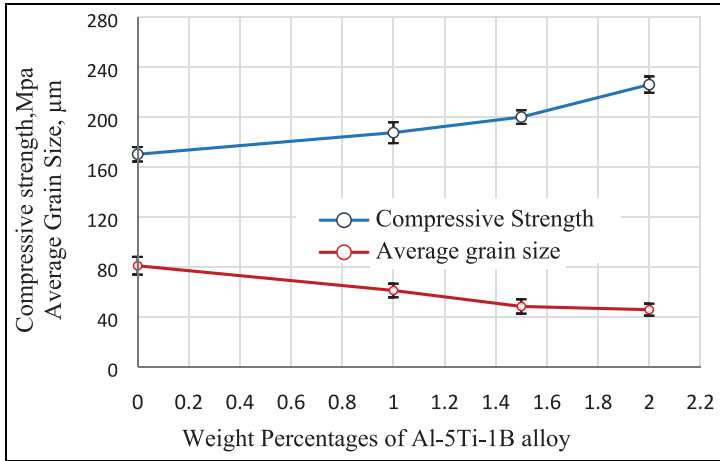


Figure 2. XRD traces for Al–5Ti–1B grain refiner in the present study.



**Figure 3.** Optical micrographs of the microstructure of Al–Mg–Si alloy with different percentages of Al–5Ti–1B grain refiner at higher magnifications  $\times 400$ : (a) 0%, (b) 1%, (c) 1.5%, and (d) 2%.

for the Al–Mg–Si alloy with different percentages of GR alloy. From this figure, it is evident that the compressive strength of the Al–Si–Mg alloy was enhanced with the addition of the GR alloy. The compressive strength increased from 171 MPa to 227 MPa with the increase of the GR alloy from 0% up to 2%. This was attributed to the creation of relatively small size grains and enhancement in the structure morphology from coarse-dendritic structure to relatively fine-equiaxed grains as shown in Figure 4. This was observed and evidenced in SEM micrographs shown in Figure 5(a)–(c). The grain size of the matrix was reduced from 82 to 46  $\mu\text{m}$  by the addition of GR alloy. The grain boundary can be used as a barrier for dislocation slip and dislocation source movement.<sup>15</sup> As the grain size reduces, the grain boundary increases, then more noticeable the grain boundary deformation is, which is helpful to prevent the growth and propagation of cracks.<sup>16</sup> So, fine grain strengthening can lead to the enhancement of elongation and higher compressive strength.



**Figure 4.** Compressive strength and average grain size for the Al–Mg–Si alloy with different wt.% of Al–5Ti–1B grain refiner.

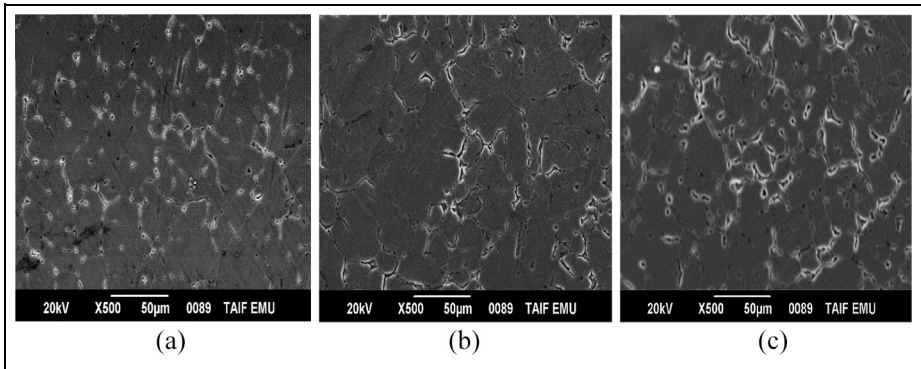


**Figure 5.** SEM shows the microstructure of the Al–Mg–Si alloy with: (a) 0% Al–5Ti–1B, (b) 1% Al–5Ti–1B, and (c) 2% Al–5Ti–1B.

### Hardness test

The bulk hardness values of the Al–Si–Mg alloy with the additions of different percentages of GR alloy are shown in Figure 6. From this figure, it is clear that the hardness was increased of Al–Si–Mg alloy with the additions of GR alloy, this is mainly due to the change in morphology of primary  $\alpha$ -Al grain from coarse dendritic structure to fine equiaxed structure.<sup>17</sup> Cibula<sup>18</sup> detected that the use of the GR alloy presents both Ti and B into the melt in the formula of  $AlB_2$ ,  $TiB_2$ , and  $Al_3Ti$ . They suggested that  $TiB_2$  particles act as insoluble substrates for primary  $\alpha$ -Al nucleation. These phases provide more nucleation sites for heterogeneous



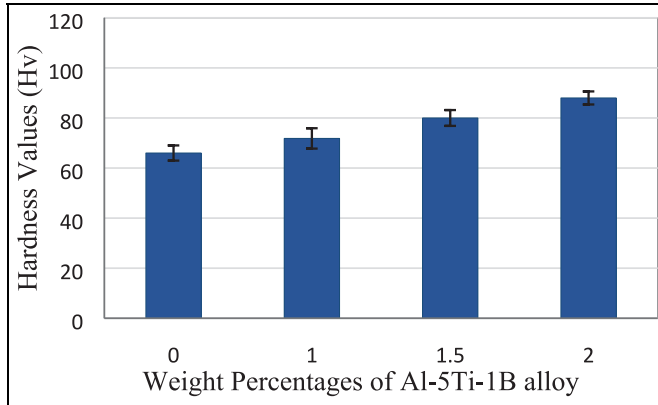


**Figure 6.** Hardness for the Al–Mg–Si alloy with different wt.% of Al–5Ti–1B grain refiner.

nucleation.<sup>19</sup> It can also be attributed to the presence of solutal titanium at the tip of the primary  $\alpha$ -Al dendrites, which controls the growth of primary  $\alpha$ -Al, hence providing more nucleation sites.<sup>20</sup>

The improvement in mechanical results due to grain refinement additions is in agreement with the previous studies. Ebrahimi et al.<sup>21</sup> studied the effect of Al–5Ti–1B refiner in addition to Al–Zn–Mg–Cu alloy, and they perceived improved mechanical properties. Pattnaik et al.<sup>17</sup> investigated the effect of Al–5Ti–1B grain refiner on the mechanical properties of 5052 Al alloy showed that the addition of Al–5Ti–1B grain refiner to the 5052 Al alloy caused a significant improvement in the mechanical properties. They suggested that the main mechanisms that led to this improvement were found to be due to the grain refinement during solidification and segregation of Ti at primary  $\alpha$ -Al grain boundaries. Farahani et al.<sup>22</sup> used Al–5Ti–1B and Al–15Zr master alloys as grain refining agents. They observed improved mechanical properties of the Zn rich Al alloy. In addition, they detected that Al–5Ti–1B is more effective than Al–15Zr in reducing the grain size.

### **Electrochemical test**

Figure 7 shows the potentiodynamic polarization curve of the Al–Mg–Si alloy with different wt.% of GR alloy specimens after corrosion test in 3.5 wt% NaCl solution. In addition, the corrosion characteristics are given in Table 1. As shown in Figure 7, all the polarization curves reveal a relatively smooth current platform in the cathodic region, which shows the reaction of oxygen reduction. It can be noted that current density increases to a certain extent, though whereas the potential increases continuously, the change in current density is less, proving the existence of an oxide layer. The corrosion current density ( $I_{\text{corr}}$ ) and corrosion potential ( $E_{\text{corr}}$ ) can be gotten by using Tafel segments of the polarization curves in Figure 7, and the results are displayed in Figure 8. Assenting to Faraday's law, it can be used



**Table 1.** The corrosion characteristics of the Al–Mg–Si alloy with different wt.% of Al–5Ti–1B grain refiner.

Sample	$\beta_a$	$\beta_c$	$R_p$ ( $\Omega \text{ cm}^2$ )	$E_{\text{corr}}$ (V)	$I_{\text{corr}}$ ( $\text{A}/\text{cm}^2$ )	CR (mpy)
0% GR	0.109	0.334	$6.488 \times 10^3$	-0.869	$2.124 \times 10^{-6}$	$2.32 \times 10^{-2}$
1% GR	0.022	1.012	$3.795 \times 10^3$	-0.656	$3.287 \times 10^{-6}$	$3.58 \times 10^{-2}$
1.5% GR	0.02	0.792	$2.591 \times 10^3$	-0.669	$3.43 \times 10^{-6}$	$3.74 \times 10^{-2}$
2% GR	0.03	0.603	$2.513 \times 10^3$	-0.689	$3.48 \times 10^{-6}$	$3.79 \times 10^{-2}$

$I_{\text{corr}}$  as a dynamic factor to describe the corrosion rate of specimens. As shown in Figure 8(a) the Al–Mg–Si alloy has the lowest  $I_{\text{corr}}$  recorded  $2.124 \mu\text{A}/\text{cm}^2$  compared to the Al–Mg–Si alloy with different wt.% of GR alloy specimens. The Al–Mg–Si alloy with 2 wt.% of GR alloy specimen recorded the highest  $I_{\text{corr}}$  ( $3.48 \mu\text{A}/\text{cm}^2$ ). The values of  $E_{\text{corr}}$  for the Al–Mg–Si alloy specimen are more negative than those of the Al–Mg–Si alloy with different wt.% of GR alloy specimens as shown in Figure 8(b). The current results are in agreement with the literature<sup>13,14,23,24</sup> that the corrosion rate increases as grain size decreases for Al alloys. The grain refinement revealed a number of grain boundaries which is act as more anodic this accelerates the dissolution of the working electrode which causes severe corrosion. The opposing view, that corrosion rate decreases as grain size decreases for aluminum, has also been presented with some studies.<sup>25–28</sup> The differences are possibly due to that corrosion response to grain-refinement induced surface reactivity depends on the exact combination of exposed environment, material, and grain refinement procedure.<sup>13</sup>

Though corrosion parameters can be determined from potentiodynamic polarization curves, the accurateness of the valued results might be compromised due to possible interference from proceeding cathodic reactions on the specimen surface. So, electrochemical impedance spectroscopy (EIS) is often used for the characterization of electrochemical interface between electrodes and electrolytes because of its advantages of sensitivity and non-destructivity.<sup>29</sup> The polarization resistance  $R_p$  for the corrosion reaction was determined and recorded in Table 1 by means of EIS measurements at the corrosion potential to assure anodic and cathodic reactions. Figure 9 shows the Bode plot containing the impedance and phase data for the Al–Mg–Si alloy with different wt.% of GR alloy. According to Figure 9 and the results recorded in Table 1, there is a tendency of decreased  $R_p$  after GR alloy addition. It is noticed that the  $R_p$  significantly decreases from about  $6.5 \text{ k}\Omega \text{ cm}^2$  for the Al–Mg–Si alloy specimen to about  $2.5 \text{ k}\Omega \text{ cm}^2$  for the Al–Mg–Si alloy with 2 wt.% of GR alloy specimen. The natural oxide layer on aluminum and its alloys generally impede the inherently active behavior of this metal. However, solutions that have aggressive anions, such as  $\text{Cl}^-$ , cause pit initiation, resulting in a quick increase of the current density at a certain potential.<sup>30</sup>

Figure 10 shows the micrographs of the Al–Mg–Si alloy with different wt.% of GR alloy specimens after immersion in 3.5 wt% NaCl solution. As indicated in this

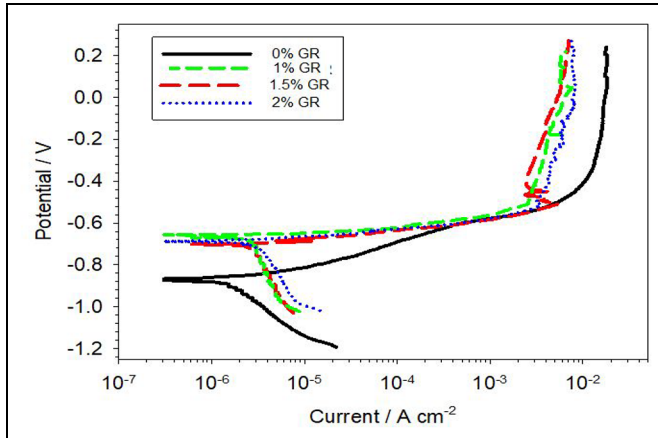


**Figure 7.** Potentiodynamic polarization curves of the Al-Mg-Si alloy with different wt.% of Al-5Ti-1B grain refiner specimens during immersion in 3.5 wt% NaCl solution.

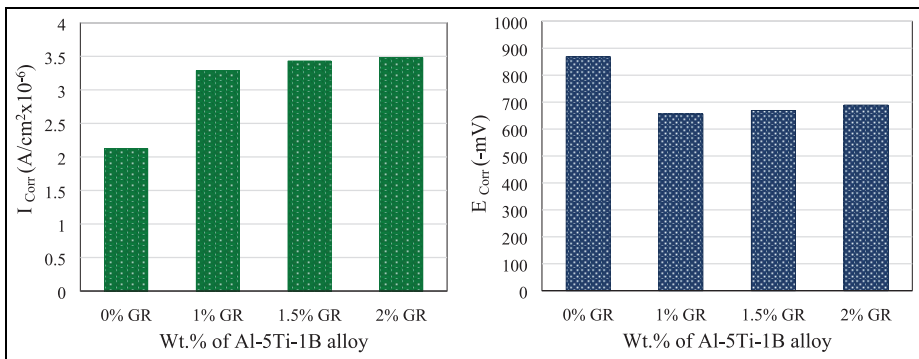


**Figure 8.** Effect of wt.% of Al-5Ti-1B grain refiner on (a) corrosion current density ( $I_{corr}$ ), (b) corrosion potential ( $E_{corr}$ ).

figure, the corroded surface showed a localized attack. The numerous cavities presented an irregular shape, suggesting that the corrosion process initiated and proceeded in the Al-matrix around the intermetallic particles. Furthermore, Figure 10(b) to (d) clearly shows a corrosive attack increased by GR alloy addition. The increase in pitting corrosion clearly visible by comparing Figure 10(a), and Figure 10(b) to (d), could explain the reduction of  $R_p$  and the corresponding increase in  $I_{corr}$  as a function of wt.% of GR alloy addition. Some studies on Al-Si alloys have stated that finer dendritic structures higher corrosion rate than coarser dendritic structures, and that this is associated with the microstructure of the interdendritic eutectic mixture.<sup>31,32</sup> Osório et al.<sup>33</sup> have recently stated that a noteworthy

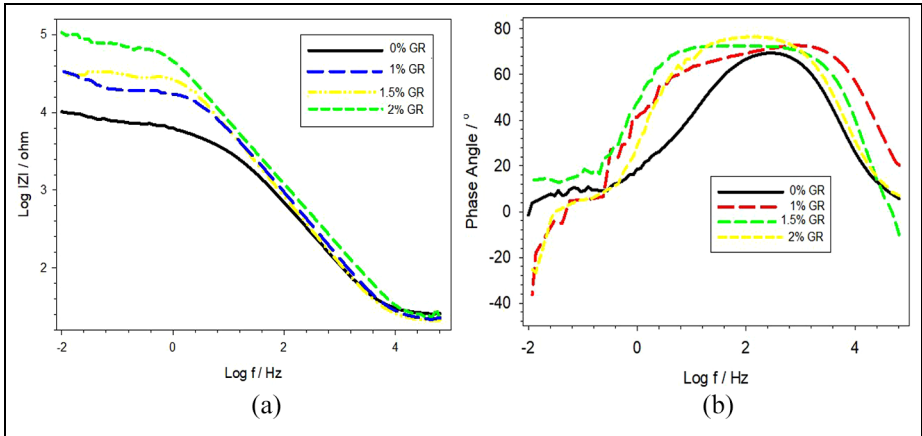


**Figure 9.** Bode plot (a, b) for the Al-Mg-Si alloy with different wt.% of Al-5Ti-1B grain refiner specimens during immersion in 3.5 wt.% NaCl solution.

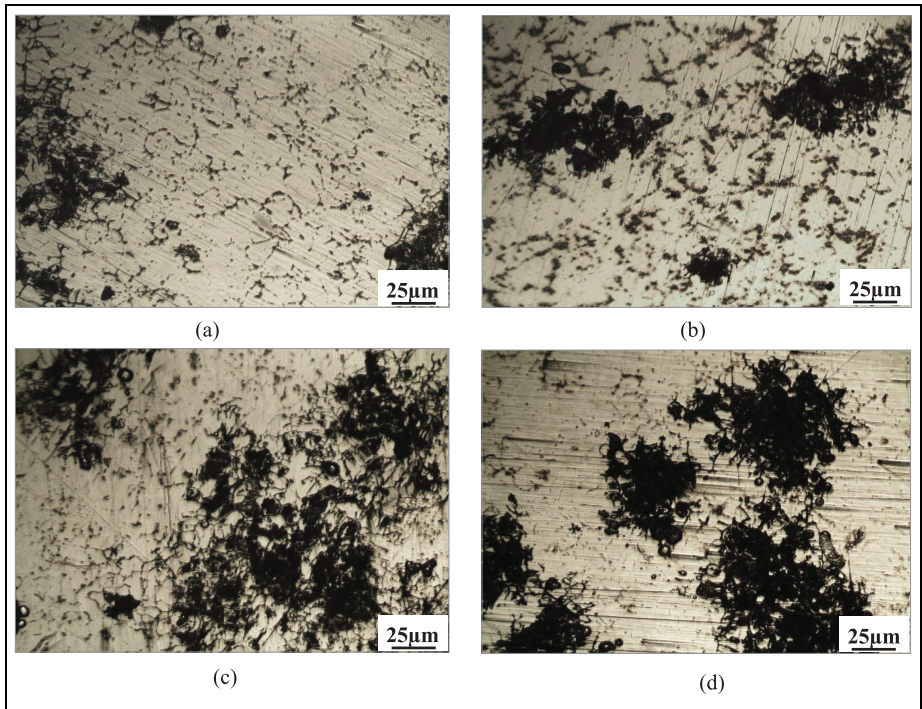


**Figure 10.** Microstructure of the Al-Mg-Si alloy with different wt.% of Al-5Ti-1B grain refiner (GR) specimens after corrosion test in 3.5 wt.% NaCl solution: (a) 0 wt% GR, (b) 1% GR, (c) 1.5% GR, and (d) 2% GR.

microstructural refinement reduced the corrosion resistance in sulfuric acid and sodium chloride solutions. The boundaries are improperly adapted due to a certain deformation in the atomic level, essentially on the Al-rich phase side of the interface since Si grows from the melt in a faceted manner) while the  $\alpha$ -Al phase solidifies with surfaces that are rough. Such localized deformation induces an increase in the corrosive action for very fine microstructures.<sup>32,33</sup> The secondary phases (intermetallic phases) distribute around the tips of aluminum dendrites and leads to differences in chemical composition at the grain boundaries. This may lead to corrosion of the areas around these grain boundaries as pitting corrosions. The presence of intermetallic phases with alloy elements of boron, titanium, magnesium, and silicon, also leads to the corrosion potential difference between intermetallic phases and aluminum phases, which results in galvanic corrosion and further intergranular corrosion.<sup>24,34</sup>

## Conclusion

The Al–Mg–Si alloy is important in many applications, such as automotive, food industry and structural applications. In the present study, the effect of Al–5Ti–1B grain refiner alloy (GR alloy) on microstructure, mechanical properties and corrosion behavior of the Al–Mg–Si alloy was considered. Based on the experimental results, it can be concluded that the grain size of the Al–Mg–Si alloy was reduced from 82 to 46  $\mu\text{m}$  by the addition of GR alloy. The morphology of  $\alpha$ -Al dendrites changes from coarse dendritic structure to fine equiaxed grains due to the addition of GR alloy and segregation of Ti, which controls the growth of primary  $\alpha$ -Al. In addition, the second phase particles of  $\text{TiAl}_3$  and  $\text{TiB}_2$  are dispersed in the aluminum matrix homogeneously. The mechanical properties of the Al–Mg–Si alloy were improved by GR alloy addition. With increasing of GR alloy from 0% to 2% wt.% GR, the compressive strength increased from 171 MPa to 227 MPa. As well as the hardness increased from 66 to 88 Hv. Otherwise, the addition of GR alloy did not reveal any marked improvements in the corrosion properties of Al–Mg–Si alloy. This because the grain refinement revealed a number of grain boundaries, which is act as more anodic. This may accelerate the dissolution of the working electrode and causes severe corrosion. The Al–Mg–Si alloy has the lowest  $I_{\text{corr}}$  recorded 2.124  $\mu\text{A}/\text{cm}^2$ . While the Al–Mg–Si alloy with 2 wt.% of GR alloy specimen recorded the highest  $I_{\text{corr}}$  (3.48  $\mu\text{A}/\text{cm}^2$ ).

## Acknowledgement

The authors would like to thank Taif University for its financial support.


## Declaration of conflicting interests


The author(s) declared no potential conflicts of interest with respect to the research, authorship, and/or publication of this article.

## Funding

The author(s) disclosed receipt of the following financial support for the research, authorship, and/or publication of this article: This research was fully funded by the Deanship of Scientific Research, Taif University, KSA [Research group number 1-441-92].

## ORCID iDs

Hafiz T Ali  <https://orcid.org/0000-0002-7095-7321>

Dalia Saber  <https://orcid.org/0000-0002-7349-1723>

## References

1. Adeosun SO, Akpan EI and Balogun SA. Wrought aluminium alloy corrosion propensity in domestic food cooking environment. *ISRN Corros* 2012; 2012: 1–6.
2. Balogun SA, Esezobor DE and Adeosun SO. Stress corrosion cracking of cast 6063 and deep drawn 1017 aluminum utensils in lycopersicum esculentum. *J Mater Eng Perform* 2007; 16: 720–725.
3. Birol Y. AlB3 master alloy to grain refine AlSi10Mg and AlSi12Cu aluminium foundry alloys. *J Alloys Compd* 2012; 513: 150–153.
4. Abd El-Aziz K, Saber D and Sallam HEM. Wear and corrosion behavior of Al–Si matrix composite reinforced with Alumina. *J Bio- Tribo-Corros* 2015; 1: 5.
5. Guan R-G and Tie D. A review on grain refinement of aluminum alloys: progresses, challenges and prospects. *Acta Metall Sin (Engl Lett)* 2017; 30(5): 409–432.
6. Saber D, Abdel-Karim R, Kandel AA, et al. Corrosive wear of alumina particles reinforced Al–Si alloy composites. *Phys Met Metall* 2020; 121(2): 197–203.
7. Zhao J, Shi M, Wang Z, et al. Effect of a new grain refiner (Al–Ti–Mg–Ce) on hardness, tensile, and impact properties of Al–7Si alloy. *Metals* 2019; 9: 228.
8. Kodetová V, Vlach M, Kudrnová H, et al. Annealing effects in commercial aluminium hot-rolled 7075(–Sc–Zr) alloys. *J Therm Anal Calorim* 2020; 142: 1613–1623.
9. Zhang Y, Yan F, Zhao YH, et al. Effect of Ti on microstructure and mechanical properties of die-cast Al–Mg–Zn–Si alloy. *Mater Res Express* 2020; 7: 036526.
10. Abd El-Aziz K and Alogla A. Experimental investigation on the behavior of AlSiMgMn alloy inoculated by Al–5Ti master alloy and fabricated by die-casting with different mold wall thicknesses. *Int J Eng Res Technol* 2020; 13(7): 1764–1774.
11. Ding W, Xia T and Zhao W. Performance comparison of Al–Ti master alloys with different microstructures in grain refinement of commercial purity aluminum. *Materials* 2014; 7: 3663–3676.
12. Pio LY, Sulaiman S, Hamouda AM, et al. Grain refinement of LM6 Al–Si alloy sand castings to enhance mechanical properties. *J Mater Process Technol* 2005; 162–163: 435–441.
13. Ralston KD, Birbilis N and Davies CHJ. Revealing the relationship between grain size and corrosion rate of metals. *Scr Mater* 2010; 63: 1201–1204.
14. Ralston KD and Birbilis N. Effect of grain size on corrosion: a review. *Corrosion* 2010; 66(7): 075005.
15. Chen F, Chen Z, Mao F, et al. TiB2 reinforced aluminum based in situ composites fabricated by stir casting. *Mater Sci Eng A* 2015; 625: 357–368.
16. Zhang SL, Yang J, Zhang BR, et al. A novel fabrication technology of in situ TiB2/6063Al composites: high energy ball milling and meltin situreaction. *J Alloys Compd* 2015; 639: 215–223.

17. Pattnaika AB, Das S, Jha BB, et al. Effect of Al-5Ti-1B grain refiner on the microstructure, mechanical properties and acoustic emission characteristics of Al5052 aluminium alloy. *J Mater Res Technol* 2015; 4(2): 171–179.
18. Cibula A. Discussion of the mechanisms of grain refinement in dilute aluminium alloys. *Metall Trans* 1972; 3: 751–753.
19. Emamy M, Daman AR, Taghiabadi R, et al. Effects of Zr, Ti and B on structure and tensile properties of Al-10Mg alloy (A350). *Int J Cast Met Res* 2004; 17: 1–17.
20. Easton M and Stjohn D. Grain refinement of aluminium alloys: Part II. Confirmation of, and a mechanism for, the solute paradigm. *Metall Mater Trans A* 1999; 30: 1625–1633.
21. Ebrahimi SS, Aghazadeh J, Dehghani K, et al. The effect of Al-5Ti-1B on the microstructure, hardness and tensile properties of a new Zn rich aluminium alloy. *Mater Sci Eng A* 2015; 636: 421–429.
22. Farahani MV, Emadoddin E, Emamy M, et al. Effect of grain refinement on mechanical properties and sliding wear resistance of extruded Sc-free 7042 aluminum alloy. *Mater Des* 2014; 54: 361–367.
23. Gollapudi S. Grain size distribution effects on the corrosion behaviour of materials. *Corros Sci* 2012; 62: 90–94.
24. Akiyama E, Zhang Z, Watanabe Y, et al. Effect of severe plastic deformation on the corrosion behaviour of aluminium alloys. *J Solid State Electrochem* 2009; 13: 277–282.
25. Song D, Ma AB, Jiang JH, et al. Corrosion behavior of ultra-fine grained industrial pure Al fabricated by ECAP. *Trans Nonferrous Met Soc China* 2009; 19: 1065–1070.
26. Ralston KD, Fabijanic D and Birbilis N. Effect of grain size on corrosion of high purity aluminium. *Electrochim Acta* 2011; 56: 1729–1736.
27. Son IJ, Nakano H, Oue S, et al. Effect of equal-channel angular pressing on pitting corrosion of pure aluminium. *Int J Corros* 2012; 2012: 450854.
28. Hockauf M, Meyer LW, Nickel D, et al. Mechanical properties and corrosion behaviour of ultrafine-grained AA6082 produced by equal-channel angular pressing. *J Mater Sci* 2008; 43: 7409–7417.
29. Nie M, Wang CT, Qu M, et al. The corrosion behaviour of commercial purity titanium processed by high-pressure torsion. *J Mater Sci* 2014; 49: 2824–2831.
30. Hockauf M, Meyer LW, Nickel D, et al. Mechanical properties and corrosion behavior of ultrafine-grained AA6082 produced by equal-channel angular pressing. *J Mater Sci* 2008; 43: 7409–7417.
31. Osório WR, Goulart PR and Garcia A. Effect of silicon content on microstructure and electrochemical behavior of hypoeutectic Al-Si alloys. *Mater Lett* 2008; 62: 365–369.
32. Goulart PR, Osório WR, Spinelli JE, et al. Dendritic microstructure affecting mechanical properties and corrosion resistance of an Al-9 wt% Si alloy. *Mater Manuf Process* 2007; 22: 328–332.
33. Osório WR, Cheung N, Spinelli JE, et al. Microstructural modification by laser surface remelting and its effect on the corrosion resistance of an Al-9 wt%Si casting alloy. *Appl Surf Sci* 2008; 254: 2763–2770.
34. Brunner JG, Birbilis N, Ralston KD, et al. Impact of ultrafine-grained microstructure on the corrosion of aluminium alloy AA2024. *Corros Sci* 2012; 57: 209–214.

## Author biographies

Khaled Abd El-Aziz is Associate Professor, Department of Mechanical Engineering, College of Engineering, Taif University, Saudi Arabia. His research interests include; materials science and engineering, mechanical testing of materials, physical metallurgy, nanotechnology, corrosion and corrosion protection, manufacturing technology (metallic alloys and composites), advanced materials, composite materials, heat treatment of ferrous and non-ferrous alloys, metal casting.

Emad M Ahmed is Professor, Department of Physics, College of Science, Taif University, Saudi Arabia. He is member of DFG Germany and member of Solid State Physics Society of Egypt. His research interests include; solid-state physics, superconductivity, structural and physical properties of metallic alloys, thermal analysis, electrical measurements such as: resistivity, internal friction.

Abdulaziz H Alghtani is Assistant Professor, Department of Mechanical Engineering, College of Engineering, Taif University, Saudi Arabia. Head of Mechanical Engineering Department College of Engineering, Taif University. His research interests include; analysis and optimization in sheet metal forming, metal forming, manufacturing technology, mechanics of materials, finite element analysis using ABAQUS program.

Bassem F Felemban is Assistant Professor, Department of Mechanical Engineering, College of Engineering, Taif University, Saudi Arabia. He is Member of MOMRG Group, University of Central Florida for 4 years. His research interests include; testing and modeling of thermo-mechanical fatigue, fatigue life design for sheet metals, manufacturing technology, friction stir welding, mechanics of materials, materials characterization.

Hafiz T Ali is Associate Professor, Department of Mechanical Engineering, College of Engineering, Taif University, Saudi Arabia. He is Member in American Society for Composites (ASC). His research interests include; design, manufacture and analysis of adhesively bonded joint behavior under mixed mode conditions, advanced manufacturing technology, composites materials, multiaxial testing.

Mona Megahed is Associate Professor of Mechanical Design and Production Engineering, Faculty of Engineering, Zagazig University. Her research interests include; manufacturing of nanopolymeric composite materials, studying static and dynamic behavior of nanopolymeric composite materials, Nano-Reinforcement effects on the properties of composite structures, hybridization effects on the properties of composite structures.

Dalia Saber is Associate Professor, Industrial Engineering Program, Department of Mechanical Engineering, College of Engineering, Taif University, Saudi Arabia. Her research interests include; materials science and engineering, advanced materials, corrosion and corrosion protection, heat treatment of ferrous and non-ferrous alloys, composite materials (PMCs and MMCs), manufacturing technology, materials characterization, nanotechnology, metal casting.